Mathematical modeling of metal ion homeostasis and signaling systems

Cui, J.

Publication date
2009

Chapter 2 The 1st Model for Yeast Calcium Homeostasis[5]

2.1 Introduction

As mentioned before, biological cells use highly regulated homeostasis system to keep a very low cytosolic Ca^{2+} level (see Section 1.3.3). The cytosolic Ca^{2+} concentration in normal yeast cell (*Saccharomyces cerevisiae*) is maintained in the range of 50-200 nM in the presence of environmental Ca^{2+} concentrations ranging from <1μM to >100mM [145]. This homeostatic process has two basic characteristics:

- "zero" steady-state error to extracellular stimuli, which means that cytosolic Ca^{2+} concentration is tightly controlled.
- Robustness of such "perfect" adaptation, which means that the system is relatively insensitive to specific kinetic parameters [119].

The underlying mechanism of this calcium homeostatic process involves the regulated internalization and sequestration of Ca^{2+} into a variety of intracellular compartments such as the vacuole, ER (endoplasmic reticulum) and Golgi apparatus through many membrane transport proteins (including channels and transporters) [4,27] (see Fig. 2.1a). Under normal conditions, extracellular Ca^{2+} enters the cytosol through an unknown Transporter X [132] whose encoded gene has not been identified yet. Cytosolic Ca^{2+} can be pumped into ER and Golgi through Pmr1 and can be sequestered into the vacuole through Pmc1 and Vcx1. Channel Cch1-Mid1 on the plasma membrane opens only under some abnormal conditions such as depletion of secretory Ca^{2+} [132], pheromone stimulation [150] and hypotonic shock [17]. Under the abnormal condition of extracellular hypertonic shock, the vacuole can release Ca^{2+} into the cytosol through Yvc1 [165]. Both the expression and function of *PMC1*, *PMR1* and *VCX1* are regulated by calcineurin, a highly conserved protein phosphatase that is activated by Ca^{2+}-bound calmodulin [51,111,223].

[5] This Chapter is based on: Jiangjun Cui and Jaap Kaandorp, Mathematical modeling of calcium homeostasis in yeast cells, *Cell Calcium* 39: 337-348, (2006).

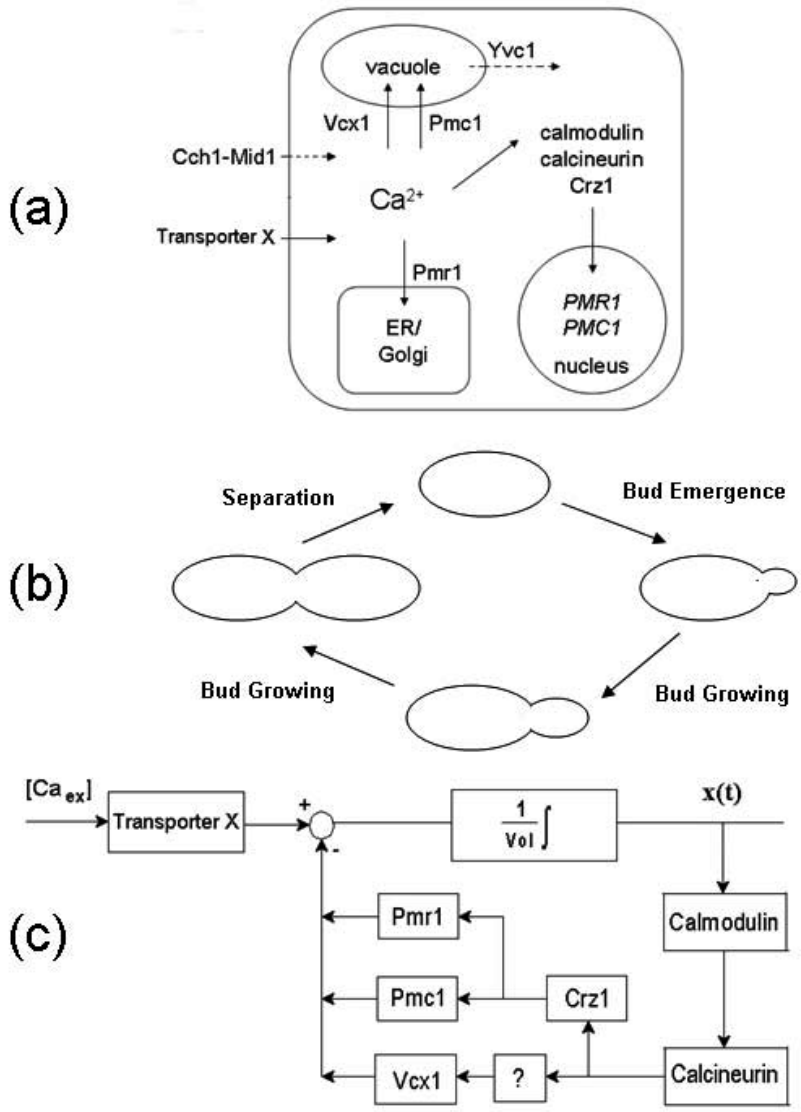

Figure. 2.1. Two schematic graphs and the block diagram of yeast calcium homeostasis system. (a) A schematic graph illustrating the protein level observations. (b) A schematic graph of the cell cycle of *Saccharomyces cerevisiae*. The bud emerges from a selected site of the cell and the further cell growth is restricted to the bud as the cell orchestrates the duplication and segregation of its organelles [173]. When the bud grows to nearly the same size of the mother cell, separation happens between the mother and daughter (i.e., the bud). (c) Control block diagram of calcium homeostasis under normal conditions. Extracellular Ca^{2+} enters the cytosol through an unknown Transporter X. The feedback control is added on Pmr1, Pmc1 and Vcx1 through calmodulin and calcineurin. Crz1 is a transcriptional factor and `?' denotes some unknown mechanism. $[Ca_{ex}]$ denotes extracellular

calcium ion concentration, $x(t)$ denotes cytosolic calcium ion concentration and Vol denotes the volume of the cytosol.

Calmodulin is a small Ca^{2+}-binding protein. In resting cells, calmodulin exists in the Ca^{2+}-free (also named apo-calmodulin) form. In response to the elevation of cytosolic Ca^{2+} level, calmodulin binds Ca^{2+} to activate a host of target proteins including calcineurin [53]. Structural analyses show that calcineurin is a heterodimer composed of a catalytic (A) subunit and an essential regulatory (B) subunit which have been highly conserved through evolution. Activated calcineurin increases the sequestering rates of Pmc1 and Pmr1 through a transcription factor Crz1. Activated calcineurin also decreases the sequestering rate of Vcx1 by regulating its synthesis [51,111].

Crz1 is a highly phosphorylated protein that can be dephosphorylated by activated calcineurin and this dephosphorylation promotes the translocation of Crz1 into the nucleus (to regulate the transcription of relevant genes including *PMC1* and *PMR1*) by increasing the efficiency of its nuclear import and down-regulating its nuclear export [29,208]. This mechanism of Crz1 translocation in yeast cells is strikingly similar to NFAT (nuclear factor of activated T-cells, a transcription factor that is also regulated by calcineurin) translocation in mammalian T-cells [29,161,208].

The so called conformational switch model was firstly proposed by Okamura *et al.* (2000), based on their detailed experimental study of NFAT1 phosphorylation states using a combination of mass spectrometry and systematic mutational analysis [161]. Later Salazar *et al.* [183] further developed this concept into a fully mathematical form which may generally apply to highly phosphorylated proteins. In the subsequent modeling we will use this mathematical model to simulate Crz1 translocation.

Saccharomyces cerevisiae is also called budding yeast and it grows by budding and dividing [173,230] (see Fig. 2.1b). The cell division cycle begins with a single unbudded cell. This cell buds, the bud grows to nearly the size of the mother cell, the nucleus divides, and the mother and daughter cells separate into two unbudded cells. The cycle then begins again for both of the cells. Intracellular organelles such as mitochondria, the vacuole, the Golgi, peroxisomes and the peripheral ER are all partitioned via specific mechanisms in this budding and dividing process [173,232] which eventually results in an exponential increase in the number of cells with a doubling time equal to the mean cell-division-cycle time [230]. The pattern of cell volume increase during cell growth is largely exponential [235]. Varying the Ca^{2+} in the growth medium from 1μM to 100mM has little effect on the growth rate of yeast cells [63]. The growth behavior of yeast cultures grown in a closed environment will experience the lag phase, logarithmic phase, stationary phase and the death phase [230].

Mutant cells lacking different genes can exhibit different phenotypes. *PMC1* null mutant cell (also denoted as *PMC1*Δ) is viable in low calcium media and fails to grow in media containing high levels of calcium ion [50] whereas *VCX1*Δ is viable in both low and high calcium media [146].

It is well-known that in plant cells, the excess cytosolic calcium ion can be extruded through pumps and exchangers on the plasma membrane [184,185]. But for yeast cells, it is not the case. Calcium efflux is truly observed in real yeast cells [90], however, there is no Ca^{2+}-ATPase or exchanger detected on the plasma membrane [212,244]. The calcium ion in the non-exchangeable pool (i.e., the vacuole) is mainly diluted by the exponential growth of yeast cells since the vacuole calcium efflux into the cytosol *in vivo* is proved to be very small under normal conditions [63]. The calcium efflux from the real cells is thought to be via exocytosis: Ca^{2+} in ER/Golgi is wrapped into secretory vesicles which will eventually fuse with the plasma membrane to free their content. Recently there has been some experimental evidence to support this hypothesis [244].

Although much has been known about the regulation mechanism of calcium homeostasis in yeast cells and there are also some experimental data available, there is no quantitative model yet to describe this important cellular process. The aim of this chapter is to present the first preliminary mathematical model of calcium homeostasis in normally growing yeast cells which is consistent with many available experimental observations. Such model can be used to steer the further experiments for acquiring more missing data and eventually help us to thoroughly understand the underlying mechanisms of calcium homeostasis, which can be a good starting point for revealing the mechanisms of a lot of related cellular processes such as calcium signaling and Zn^{2+} homeostasis [135].

2.2 Methods

2.2.1 Control Block Diagram

Based on the protein level observations and relevant experimental results about the feedback regulation part, we can first build the control block diagram of the calcium homeostasis problem as shown in Fig. 2.1c.

In this diagram, we can see that under normal conditions, if we let the inflow rate through Transporter X into the cytosol subtract the sequestering rates of Pmc1, Pmr1 and Vcx1, then we can immediately get the change rate of cytosolic Ca^{2+}. For non-growing cells, if we take an integral of this change rate and divide it by the volume of the cytosol, then eventually we will get the concentration of cytosolic Ca^{2+} (i.e., $x(t)$). In the case of growing cells, we need to further consider the dilution effect caused by the cell growth.

The mathematical modeling of calcium homeostasis in yeast cells under normal conditions can now be divided into three parts: feedback modeling, protein modeling (including Transporter X, Pmc1, Pmr1 and Vcx1) and growth modeling.

2.2.2 Feedback Modeling

Sensing cytosolic Ca^{2+}: In yeast cells, since one of the two C-terminal EF-hands (site IV) is usually defective, yeast calmodulin can only bind to a maximum of three molecules of

Ca^{2+} [53]. For simplicity, we assume that very strong cooperativity exists among the 3 active sites, then we can describe the cytosolic Ca^{2+} sensing process as follows [93]:

$$3Ca^{2+} + Calmodulin \rightleftharpoons CaM \tag{2.1}$$

where CaM denotes Ca^{2+}-bound calmodulin. If we further denote the concentration of Ca^{2+}-bound calmodulin as $m(t)$, then according to the law of mass action, we can derive the time dependence of $m(t)$ as follows :

$$m'(t) = k_M^+([CaM_{total}] - m(t))x(t)^3 - k_M^- m(t) \tag{2.2}$$

where k_M^+ denotes the forward rate constant, k_M^- denotes the backward rate constant, $x(t)$ denotes cytosolic calcium ion concentration and $[CaM_{total}]$ denotes the total concentration of calmodulin (including Ca^{2+}-free and Ca^{2+}-bound form).

Calcineurin activation: The catalytic (A) unit of calcineurin contains a carboxyl-terminal autoinhibitory domain and upon elevation of cytosolic Ca^{2+} level, Ca^{2+}-bound calmodulin reversibly binds to this catalytic subunit and ultimately activates calcineurin by displacing the autoinhibitory domain [46,53]. This binding process can be described as:

$$CaM + Calcineurin \rightleftharpoons CaN \tag{2.3}$$

where CaN denotes activated calcineurin. Since each molecule of calcineurin binds with one molecule of Ca^{2+}-bound calmodulin, if we denote the concentration of activated calcineurin as $z(t)$, then according to the law of mass action, we can derive the following equation:

$$z'(t) = k_N^+([CaN_{total}] - z(t))m(t) - k_N^- z(t) \tag{2.4}$$

where k_N^+ denotes the forward rate constant, k_N^- denotes the backward rate constant, $m(t)$ denotes the concentration of Ca^{2+}-bound calmodulin and $[CaN_{total}]$ denotes the total concentration of calcineurin (including inactive and activated). This equation will still be valid if $z(t)$ and $[CaN_{total}]$ are all expressed in relative units to a certain constant (i.e., the two sides of the above equation are simultaneously divided by a certain constant), we will make use of this observation later on.

Gene expression control: Experimental results show that activated calcineurin regulates the sequestering rates of Pmc1 and Pmr1 by controlling the synthesis of these two proteins through a transcription factor Crz1 (also named as Tcn1) [111,208]. Although it has not been totally established by experiments that only fully dephosphorylated Crz1 molecules in the nucleus are transcriptionally active, it has been shown to be the case for NFAT1 (a main member of NFAT family) [161,183]. So here we assume that it is also the case for Crz1. As mentioned in the introduction part, here we use a conformational

switch model to simulate Crz1 translocation. By describing the conformational switch model as a protein network and using the rapid equilibrium approximation [183], we can use the following equation to describe the kinetics of the total nuclear Crz1 fraction which is denoted by *h(t)*:

$$h'(t) = d \cdot \phi \cdot (1 - h(t)) - f \cdot \psi \cdot h(t) \tag{2.5}$$

where d denotes the import rate constant, f denotes the export rate constant, ϕ denotes the ratio of the fraction of the cytoslic active conformation over the total cytosolic fraction and ψ denotes the ratio of the fraction of nuclear inactive conformation over the total nuclear fraction. ϕ can be calculated as follows [183]:

$$\phi = \frac{\sum_{n=0}^{N} a_n}{\sum_{n=0}^{N} (a_n + i_n)} = \frac{1}{1 + \sum_{n=0}^{N} i_n / \sum_{n=0}^{N} a_n} = 1/(1 + L_0 \frac{(\lambda k / c)^{N+1} - 1}{\lambda k / c - 1} \frac{k/c - 1}{(k/c)^{N+1} - 1}) \tag{2.6}$$

Where the small case letters a_n and i_n $(n = 0,1,2...N)$ denote cytosolic active and inactive conformations with n phosphorylated residues respectively. k and c denote kinase and calcineurin activity in the cytosol respectively (Please note that in the remaining part of this Chapter, the capital letters A_n, I_n $(n = 0,1,2...N)$, K and C are the corresponding nuclear symbols). N is the number of relevant regulatory phosphorylation sites (In the case of NFAT1, experimental data shows that $N = 13$ [Ref. 161,183]). L_0 is the basic equilibrium constant and λ is the increment factor.

Under the assumption of $k/c = K/C$, we can calculate $\psi = 1 - \phi$. By observing the above expression, ϕ can be regarded as a function of k/c. If we assume that the kinase level is a constant and further express the concentration of activated calcineurin(i.e., $z(t)$) in dimensionless units relative to this constant (see Eq. 2.4) , then

$$\phi(k/c) = \phi(1/(c/k)) = \phi(1/z(t)) \tag{2.7}$$

Now we can rewrite the kinetics equation (Eq. 2.5) of the total nuclear fraction as follows:

$$h'(t) = d \cdot \phi(1/z(t)) \cdot (1 - h(t)) - f \cdot (1 - \phi(1/z(t))) \cdot h(t) \tag{2.8}$$

where ϕ represents the function
$\phi(y) = 1/(1 + L_0 \cdot ((\lambda y)^{N+1} - 1)/(\lambda y - 1) \cdot (y - 1)/(y^{N+1} - 1))$.

Once we know the total nuclear fraction $h(t)$, we can further calculate the transcriptionally active Crz1 fraction in the nucleus as follows[6] [183]:

$$A_0 + I_0 = h(t) \cdot \frac{A_0 + I_0}{\sum_{n=0}^{N}(A_n + I_n)} = \frac{h(t) \cdot (1 + L_0)}{\frac{(K/C)^{N+1} - 1}{K/C - 1} + L_0 \frac{(\lambda K/C)^{N+1} - 1}{\lambda K/C - 1}} \tag{2.9}$$

Under the assumption of $k/c = K/C$, we can rewrite the above expression as

$$A_0 + I_0 = h(t) \cdot \theta(k/c) = h(t) \cdot \theta(1/z(t)) \tag{2.10}$$

where $z(t)$ is in dimentionless units relative to the cytosolic kinase level which is assumed to be constant and the function
$\theta(y) = (1 + L_0)/((y^{N+1} - 1)/(y - 1) + L_0 \cdot ((\lambda y)^{N+1} - 1)/(\lambda y - 1))$..

Once we know the transcriptionally active Crz1 fraction in the nucleus, since Crz1 is a transcription factor which is necessary for the synthesis of Pmc1 and Pmr1, a natural assumption is that the concentrations of these two proteins are proportional to transcriptionally active Crz1 fraction in the nucleus which means that:

$$[Pmc1] = k_a \cdot h(t) \cdot \theta(1/z(t)) \tag{2.11}$$

$$[Pmr1] = k_b \cdot h(t) \cdot \theta(1/z(t)) \tag{2.12}$$

where $[Pmc1]$ and $[Pmr1]$ denote the concentrations of Pmc1 and Pmr1 respectively and k_a, k_b denote the feedback control constants.

For the feedback regulation of activated calcineurin on the synthesis of Vcx1, we do not know exactly what is going on there. The only knowledge about this regulation is that the mechanism is possibly posttranslational and the general effect is suppressing [51]. So here we use a highly putative expression to model this regulation as follows:

$$[Vcx1] = k_d /(1 + k_c \cdot z(t)) \tag{2.13}$$

where k_c, k_d denote the feedback control constants. With this expression the suppressing relation (i.e., when $z(t)$ rises, the concentration of Vcx1 will drop) can be represented.

2.2.3 Growth Modeling

As mentioned before, yeast cells grow by budding and dividing [173,230]. Normal yeast cells are somewhat spherical with a typical diameter of 1-7μm [230], so we can assume

---

[6] Please note that $h(t) = \sum_{n=0}^{N}(A_n + I_n)$, which means that the total nuclear fraction is the sum of the fractions of all the nuclear inactive and active conformations.

our mode cell (without growth) as a sphere with a diameter of 4μm. Since the pattern of cell volume growth is largely exponential [235], it is plausible to model the volume growth as follows (C.L. Woldringh, personal communication):

$$V(t) = V_0 \cdot e^{\alpha t} \tag{2.14}$$

where $V(t)$ denotes the volume of the cell (Please note for $nT \le t \le (n+1)T$, $n = 1,2,3,...,$ the original cell has divided into 2^n cells and *V(t)* is the sum of the volumes of all these 2^n cells) , V_0 denotes the initial volume (33.5 μm^3), T is the mean cell-division-cycle time and α denotes the growth rate constant which can be calculated as $\ln 2 / T$. Since the intracellular organelles are all partitioned during cell growth [173,232], we assume that the volume growth of the organelles (the vacuole, ER and Golgi, etc.) follows the same exponential pattern [44]. Two obversations worthy of notice are that the diameter of the neck area between the mother cell and the bud is much smaller than the size of the mother cell (see Fig. 2.1b) and that the duration of the unbudded period is much shorter than the mean cell-division-cycle time [235]. To calculate the surface area of the cell (including the bud), we can consider an approximating case of the bud sphere growing separately from the mother cell with the total volume bound by the above exponential growth relation (i.e., the volume of the bud $V_b = V_0(e^{\alpha t} - 1)$ for $0 \le t < T$). With this approximation, the surface area of the cell (including the bud) can be calculated as follows:

$$S(t) = S_0 \cdot 2^n \cdot (1 + (e^{\alpha(t-nT)} - 1)^{2/3}) \quad (nT \le t < (n+1)T, n = 0,1,2,3,...) \tag{2.15}$$

where $S(t)$ denotes the surface area of the cell (Please note again that for $nT \le t < (n+1)T, n = 0,1,2,3,...$, the original cell has divided into 2^n cells and $S(t)$ is the sum of the surface areas of all these 2^n cells), S_0 denotes the initial surface area (50.3 μm^2). Under normal conditions, yeast cells will double every 1.5-2.5 hours [63,230]. With such growth rate, it is easy to show that $1 \le (S(t)/S_0)/(V(t)/V_0) < 1.12$ which means that the cell surface area change is roughly proportional to the cell volume change during budding and dividing. So approximately we can use an exponential growth model (similar as Eq. 2.14) instead of using Eq. 2.15 to describe the surface area change of the cell (also to describe membrane surface area change of the organelles) during cell growth. As we will see, such an approximation will make our preliminary model much simpler.

2.2.4 Protein Modeling

Experimental results show that the uptake of all the four involved proteins (Transporter X [132], Pmc1 [215], Pmr1 [205] and Vcx1 [159]) conforms to the Michaelis-Menten equation, which is a general equation for describing single site protein-mediated ion uptake [5]. Moreover, since yeast cells are growing, a natural assumption is that during growth, the uptake rate of calcium transporting protein is proportional to the surface area

of the corresponding membrane on which this protein resides. For example, the uptake rate of Transporter X can be expressed as :

$$U(t) = \frac{V_{\max} \cdot [Ca_{ex}]}{K_x + [Ca_{ex}]} \cdot e^{\alpha t} \tag{2.16}$$

where $U(t)$ denotes the uptake rate of Transporter X, $[Ca_{ex}]$ denotes extracellular calcium ion concentration, $V_{\max}$ is the maximum uptake rate of Transporter X and K_x is the binding constant.

2.2.5 Preliminary Model

Since now we have built the uptake models for all the four involved proteins and models for the relevant feedback regulation, according to the control block diagram (Fig. 2.1c) and by further considering the dilution effect caused by the exponential cell growth, we can derive the main equation of our calcium homeostasis problem as follows:

$$\begin{aligned} x'(t) = & \underbrace{\frac{V_x \cdot [Ca_{ex}]}{K_x + [Ca_{ex}]}}_{TransporterX} - \underbrace{h(t)\theta(1/z(t))\frac{V_1 \cdot x(t)}{K_1 + x(t)}}_{Pmc1} - \underbrace{h(t)\theta(1/z(t))\frac{V_2 \cdot x(t)}{K_2 + x(t)}}_{Pmr1} \\ & - \underbrace{\frac{1}{1 + k_c z(t)}\frac{V_3 \cdot x(t)}{K_3 + x(t)}}_{Vcx1} - \alpha x(t) \end{aligned} \tag{2.17}$$

where $x(t)$ denotes cytosolic calcium ion concentration , $z(t)$ denotes the concentration of activated calcineurin which is expressed in relative units to constant cytosolic kinase level, $h(t)$ denotes total nuclear fraction of Crz1 , α denotes the growth rate, and θ is the function $\theta(y) = (1 + L_0)/((y^{N+1} - 1)/(y - 1) + L_0 \cdot ((\lambda y)^{N+1} - 1)/(\lambda y - 1))$ (Note that in the above main equation the feedback constants k_a, k_b and k_d have been implicated in parameters V_1, V_2 and V_3 respectively, the last term (i.e., $-\alpha x(t)$) appears because the volume of the cytosol is changing during growth. According to differentiation rule, $x'(t) = (C'(t) - x(t) \cdot Vol'(t))/Vol(t)$ where $C(t)$ denotes the cytosolic Ca^{2+} content).

It is reported that after 2.5 hours of incubation, the maximum Ca^{2+} accumulation due to Transporter X is around 390nmol/10^9cells [132]. Since the cell counting is performed at the end of the assay [132] and the cell number has doubled in 2.5 hours, we can roughly calculate parameter V_x in the main equation as follows:

$$\begin{aligned} V_x &= V_{\max}/(V_0 * 10\%) = (2 * 390 nmol/10^9 cells/(\int_0^{2.5hours} e^{\alpha t} dt))/(33.5 \mu m^3 * 10\%) \\ &\approx 1000 \mu M/\min \end{aligned} \tag{2.18}$$

(Please note that here we assume the volume percentage of the cytosol to be 10% [135] and the growth rate constant $\alpha = 0.006\,\mathrm{min}^{-1}$ [63]). Then we have to consider the influence of calcium uptake by the growing yeast cells on the extracellular media calcium ion concentration. Under the most favourable conditions, yeast cells will double in number every 90 minutes until a density of 3-5*10^7 cells/ml after which the growth rate slows down [230]. So after 2.5 hours of normal growth from any initial density (obviously this density should be less than 2.5*10^7 cells/ml to assure normal log-phase growth), the upper limit of the relative change of extracellular media calcium ion concentration can be roughly estimated as follows:

$$\frac{\Delta[Ca_{ex}]}{[Ca_{ex}]} < \int_0^{2.5h} U(t)dt * (5*10^7 cells/ml/2)/[Ca_{ex}]*100\% < 5\% \qquad (2.19)$$

(Please note that K_x is reported to be 500 μM [132]). This means the relative change rate of extracellular media calcium ion concentration is very slow and it is a good approximation to assume $[Ca_{ex}]$ as a constant. Then we look at the change of vacuolar calcium ion concentration after some hours of normal growth:

$$\Delta[Ca_{vacuole}] < \int_0^t U(y)dy/(33.5e^{\alpha t}\mu m^3 * 50\%) < \frac{1}{\alpha}V_{\max}/(33.5\mu m^3 * 50\%) < 32mM \quad (2.20)$$

(Please note that here we assume the volume percentage of the vacuole to be 50% [135] and the growth rate constant $\alpha = 0.006\,\mathrm{min}^{-1}$). If we assume that the initial vacuolar Ca^{2+} concentration to be around 2mM [63] (Please note that this original Ca^{2+} concentration will exponentially decrease due to the exponential growth of vacuolar volume), we can conclude that the influx into the vacuole will never saturate the store due to the dilution effect of cell growth. Since at least 90% of the total cellular Ca^{2+} is sequestered within the vacuole [145], we can estimate the change of calcium ion concentration in ER and Golgi after any hours of normal growth as follows:

$$\Delta[Ca_{ER\&Golgi}] < \int_0^t U(y)dy * 10\%/(33.5e^{\alpha t}\mu m^3 * 10\%) < 16mM \qquad (2.21)$$

(Please note that here we assume the volume percentage of ER and Golgi to be 10%). If we assume that the initial Ca^{2+} concentration in ER and Golgi to be less than 1mM [212] and further take into account the Ca^{2+} efflux from ER and Golgi through exocytosis, we can conclude that the Ca^{2+} saturation in the ER and Golgi will never happen due to the dilution effect of cell growth. So the main equation (Eq. 2.17), together with three previously stated equations (Eqs. 2.2, 2.4, 2.8) for $m(t)$, $z(t)$ and $h(t)$ respectively, constitutes a more or less complete mathematical model for calcium homeostasis in yeast cells under normal conditions. The whole set of parameters (except the control parameter $[Ca_{ex}]$) in our model which will be used in the subsequent simulations are listed in Table 2.1.

Table 2.1: Model parameters for which all results are calculated unless otherwise stated.[7]

Parameter	Value	Description
K_x	500 μM	the binding constant of Transporter X [132]
K_1	4.3 μM	the binding constant of Pmc1 [215]
K_2	0.1 μM	the binding constant of Pmr1 [205]
K_3	100 μM	the binding constant of Vcx1 [159]
V_x	1000 μM/min	the rate parameter of Transporter X (Calculated from [132])
V_1	30000 μM/min	the rate parameter of Pmc1
V_2	100 μM/min	the rate parameter of Pmr1
V_3	10000 μM/min	the rate parameter of Vcx1
k_c	10	the feedback control constant
k_M^+	500 $(\mu M)^{-3}min^{-1}$	the forward rate constant of Eq. 2.2
k_M^-	100 min^{-1}	the backward rate constant of Eq. 2.2
k_N^+	5 $(\mu M)^{-1}min^{-1}$	the forward rate constant of Eq. 2.4
k_N^-	5 min^{-1}	the backward rate constant of Eq. 2.4
$[CaM_{total}]$	25 μM	the total concentration of calmodulin
$[CaN_{total}]$	25	the total concentration of calcineurin
d	0.4 min^{-1}	the nuclear import rate constant [183]
f	0.1 min^{-1}	the nuclear export rate constant [183]
N	13	the number of relevant regulatory phosphorylation sites [183]
L_0	$10^{-N/2}$	the basic equilibrium constant [183]
λ	5	the increment factor [183]
α	0.006 min^{-1}	the growth rate constant [63]

2.3 Results

2.3.1 Steady-State Properties

The model consists of four equations (Eqs. 2.2, 2.4, 2.8, 2.17) with four unknowns: $x(t)$, $m(t)$, $z(t)$ and $h(t)$. By setting the zero initial conditions (except that $z(0)$ is set to be 10^{-8} to avoid the singularity) and then solving the four equations (Eqs. 2.2, 2.4, 2.8, 2.17, using the parameters listed in Table 2.1) numerically, we can first depict the $x(t)$ curves

[7] Please note that $[CaN_{total}]$ is expressed in dimensionless units relative to cytosolic kinase level which is assumed to be constant.

for parameter $[Ca_{ex}] = 1\mu M$ as shown in Fig. 2.2a. In Fig. 2.2b, resting levels of $x(t)$ for different values of parameter $[Ca_{ex}]$ are shown. In the simulations we also investigated resting levels of calcium ion-bound calmodulin. The simulated calcium ion-bound calmodulin concentration rests within 0.048-0.49μM (regardless of the initial conditions) when the simulated medium calcium level ($[Ca_{ex}]$) ranges from 1μM to 100mM. The derived figure (data not shown here) is very similar to Fig. 2.2b.

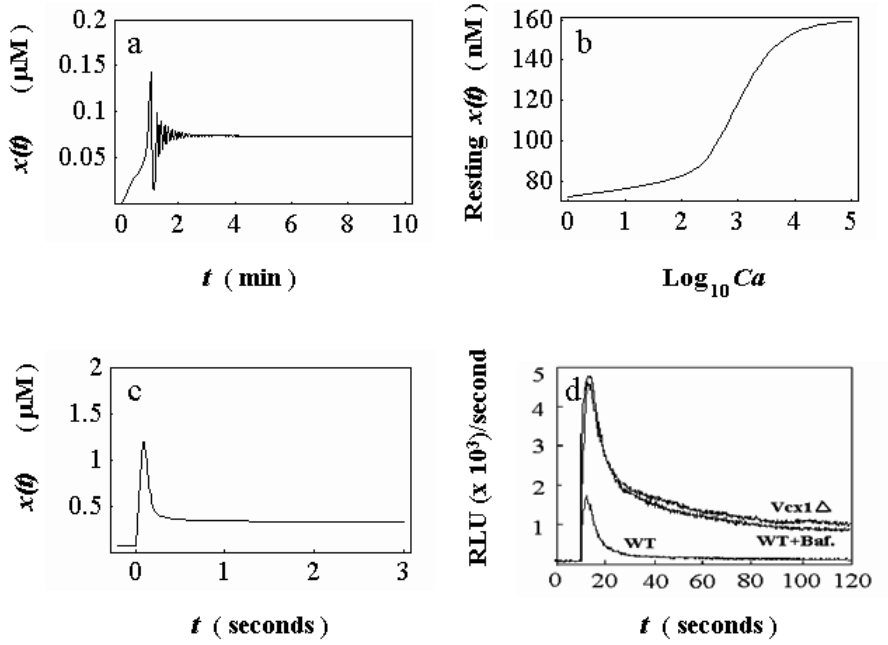

Figure. 2.2. Resting levels and comparison of response curves.
(a) $x(t)$ curve for parameter $[Ca_{ex}] = 1\mu M$ under zero initial conditions (except that $z(0)$ is set to be 10^{-8} to avoid the singularity). The simulated cytosolic calcium ion concentration eventually rests at 73nM. (b) Resting levels of $x(t)$ for different values of parameter $[Ca_{ex}]$. The simulated cytosolic calcium ion level of our model cell rests within 73-159nM (regardless of the initial conditions) when the simulated medium calcium level (parameter $[Ca_{ex}]$) ranges from 1μM to 100mM. (c) Simulated response curve of $x(t)$ under the step-like disturbance of that at $t = 0$, the simulated extracellular calcium ion level ($[Ca_{ex}]$) suddenly changes from 6μM to 100mM. (d) The corresponding experimental response curve of real cells responding to step-like disturbance in media calcium ion concentration (Figure from [146], courtesy of David M. Bedwell), WT denotes wild type cell. Stimulus condition: the extracellular calcium ion concentration is firstly controlled at a low level (~6μM) using EGTA. At $t = 10$ s, the media calcium ion level is suddenly increased to 100mM by injecting $CaCl_2$ into the cuvette. Cytosolic calcium ion concentration is reported in aequorin luminescence. RLU denotes relative luminescence unit. The curve of interest is the bottom curve which is labeled as WT curve. The top two curves in this figure show the response curves of Vcx1 mutant (labeled as Vcx1Δ) and wildtype cell pre-treated with bafilomycin A_1 (labeled as WT+Baf.), respectively.

2.3.2 Transients and Mutant Behavior

Now let us examine how our model cell will respond to extracellular stimulus. For the model cell (Eqs. 2.2, 2.4, 2.8, 2.17, using the parameters listed in Table 2.1), the stimulus condition is that at $t = 0$, the simulated extracellular calcium ion level ($[Ca_{ex}]$) suddenly changes from 6μM to 100mM. The simulated response curves of $x(t)$, $m(t)$, $z(t)$, $h(t)$ and the transcriptionally active Crz1 fraction are shown in Fig. 2.2c and Fig. 2.3(b-d) respectively, in which we can see that at first our model cell is in resting state: the simulated cytosolic calcium ion concentration $x(t)$ rests at 76nM (see Fig. 2.2c), the simulated calcium ion-bound calmodulin concentration $m(t)$ rests at 0.05μM (Fig. 2.3b) and around 47% of Crz1 molecules are in the nucleus (Fig. 2.3d). However, only 2% of all Crz1 molecules are transcriptionally active (see Fig. 2.3d). The sudden change of the simulated extracellular calcium ion level (i.e., parameter $[Ca_{ex}]$) incurs a sudden rise of the simulated cytosolic calcium ion level (Fig. 2.2c) and then calmodulin senses this elevation and binds calcium ions (Fig. 2.3b) to initiate the feedback control mechanism. As a result, the simulated concentration of activated calcineurin quickly rises from its original resting level of 1.29 to a peak value of more than 18 (Fig. 2.3c) and subsequently these activated calcineurin molecules dephosphorylate Crz1 so that the simulated transcriptionally active Crz1 fraction increases from 2% to more than 40% (Fig. 2.3d). Then due to the strong effects of feedback regulation, the simulated cytosolic calcium ion level is quickly lowered and then gradually goes to a new resting level of 159nM (Fig. 2.2c and Fig. 2.3a). Almost at the same time the simulated concentration of calcium ion-bound calmodulin decreases (more gradually) to a new resting value of 0.49μM (Fig. 2.3b) and the simulated concentration of activated calcineurin decreases (even more gradually) to a new resting value of 8.26 (Fig. 2.3c), whereas more Crz1 molecules are imported into the nucleus until that almost all Crz1 molecules are in the nucleus (Fig. 2.3d) and eventually the simulated transcriptionally active Crz1 fraction further increases gradually to a high resting level of 88% (Fig. 2.3d).

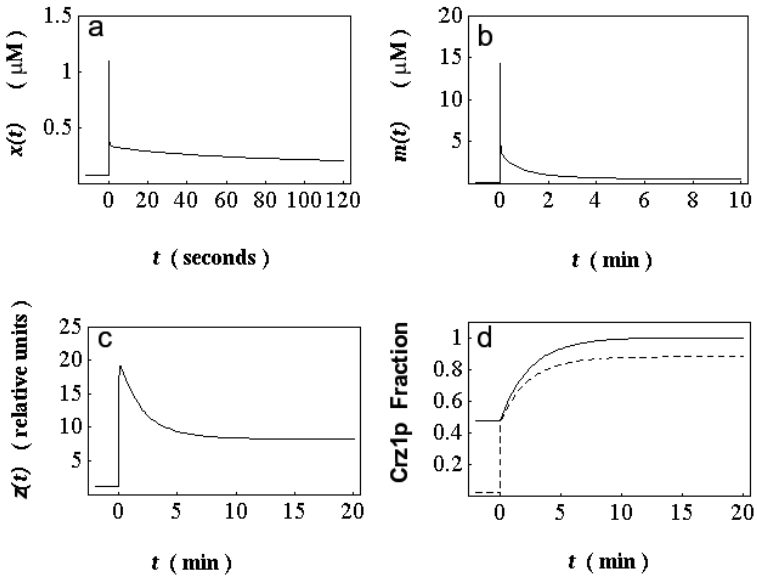

Figure. 2.3. The simulated response curves under the step-like disturbance of that at $t = 0$. The simulated extracellular calcium ion level ($[Ca_{ex}]$) suddenly changes from 6μM to 100mM. (a) Response curve of $x(t)$. This figure is the same as Fig. 2.2c except that here the curve is depicted in a longer time range. (b) Response curve of $m(t)$. (c) Response curve of $z(t)$. (d) Response curves of Crz1 fraction. The solid curve describes the response change of $h(t)$ (i.e., the total nuclear Crz1 fraction) and the dashed curve describes the response change of the transcriptionally active Crz1 fraction.

Now we would like to check the mutant behavior of our model. After taking the sequestering rate part of Pmc1 (i.e., $h(t)\theta(1/z(t))\dfrac{V_1 \cdot x(t)}{K_1 + x(t)}$) out of the main equation (Eq. 2.17), the model cell becomes a *PMC1* null mutant cell. In Fig. 2.4a and Fig. 2.4b, we depict the curves of the simulated cytosolic calcium ion concentration ($x(t)$) of our model *PMC1*Δ cell under the conditions of parameter $[Ca_{ex}] = 6\mu M$ and $[Ca_{ex}] = 200mM$ respectively. From Fig. 2.4a, we can see that in a typical low calcium media (parameter $[Ca_{ex}] = 6\mu M$), after a short transient time, the simulated cytosolic calcium ion concentration eventually rests at 82nM. From Fig. 2.4b, we can see that in a high calcium media ($[Ca_{ex}] = 200mM$), the simulated cytosolic calcium ion concentration rises quickly and almost linearly and there is no physiologically reasonable resting level anymore. In 5 minutes, the simulated cytosolic calcium ion concentration has rocketed up to a level higher than 4mM. The transition point on which the system transiting from having a reasonable resting level to having no reasonable resting level is around 60μM (data not shown here).

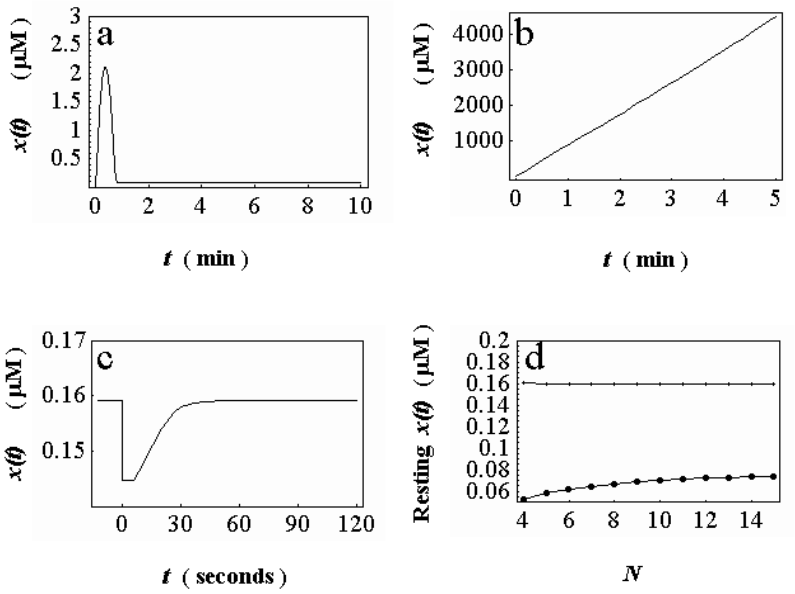

Figure. 2.4. *PMC1* null mutant behaviour and parameter sensitivity. (a) $x(t)$ curve of the simulated *PMC1* null mutant for parameter $[Ca_{ex}] = 6\mu M$ under zero initial conditions (except that $z(0)$ is set to be 10^{-8} to avoid the singularity). The simulated cytosolic calcium ion concentration eventually rests at 82nM. Further tests show this resting level is regardless of the initial conditions. (b) $x(t)$ curve of the simulated *PMC1* null mutant for parameter $[Ca_{ex}] = 200mM$. Here the resting levels for parameter $[Ca_{ex}] = 6\mu M$ are used as initial conditions. In several minutes, the simulated cytosolic calcium ion concentration has rocketed up almost linearly to a level higher than 4mM. Further analysis shows that $x(t)$ eventually rests at an unreasonably high level (143mM) which means the system is out of control. (c) $x(t)$ response curve for parameter $[Ca_{ex}] = 100mM$, at $t = 0$, k_N^+ suddenly increases from 5(μM)$^{-1}$ min^{-1} to 5000(μM)$^{-1}$ min^{-1} and at $t = 6$ seconds, it changes back to 5(μM)$^{-1}$ min^{-1}. (d) Influence of N on the simulated resting levels of $x(t)$. The upper curve (with smaller dots) depicts the resting values of the simulated cytosolic calcium ion concentration for parameter $[Ca_{ex}] = 100mM$ with N ranging from 4 to 15. The lower curve (with larger dots) depicts the simulated resting values for parameter $[Ca_{ex}] = 1\mu M$.

Similarly we can do simulations for the *VCX1* null mutant cell. Investigations show that when the simulated medium calcium level ($[Ca_{ex}]$) ranges from 6μM to 100mM, the simulated cytosolic calcium ion level of our model *VCX1*Δ cell rests within 76-159nM. Under the stimulus condition of that at $t = 0$, the simulated extracellular calcium ion level ($[Ca_{ex}]$) suddenly changes from 6μM to 100mM, the simulated $x(t)$ response curve of our model *VCX1*Δ cell is almost identical to that of the simulated wild type cell (Fig. 2.2c).

2.3.3 Parameter Sensitivity

The next issue is the robustness of our feedback control system. In the following simulation, the test condition is that parameter $[Ca_{ex}]$ is set to be 100mM and at $t = 0$, we let k_N^+ suddenly change from 5(μM)$^{-1}$ min^{-1} to 5000(μM)$^{-1}$ min^{-1} and then at $t = 6$ seconds, it changes back to 5(μM)$^{-1}$ min^{-1}. In Fig. 2.4c, we can see that at first, the simulated cytosolic calcium ion level rests at 159nM and it quickly drops to 145nM due to this large upward impulse-like disturbance, rests there for a while and then recovers to 159nM after the disturbance is over. Further tests show that when large upward or downward impulse-like disturbance is imposed on other rate constants, we can derive similar results.

As mentioned above, in our model the number of relevant regulatory phosphorylation sites (i.e., N) is put to 13, which is actually an experimentally found number for NFAT1 translocation. Since the exact value of N for Crz1 translocation has not been well established, we now would like to examine the influence of parameter N to our model cell behavior. By changing the value of N and recording the corresponding resting levels, we can eventually derive Fig. 2.4d. From this figure, we can see that for high media calcium level ($[Ca_{ex}] = 100mM$, the simulated resting level of our model cell is totally insensitive to the change of N. For low media calcium level ($[Ca_{ex}] = 1\mu M$), the simulated resting level seems to be more sensitive and increases somewhat with the increase of N.

We have tested the sensitivity of the system to every parameter except those reported ones (see Table 2.1) and Table 2.2 gives a summary of the range of the parameter values in which the system is very insensitive to the change of that particular parameter.

Table 2.2: The range of parameter values in which the system shows great insensitivity

Parameter	Value range (Min-Max)	Resting level range of $x(t)$ for $[Ca_{ex}]$ ranging from 1μM to 100mM	
		Parameter = Min	Parameter = Max
V_1	25000-5000000 μM/min	73-185 nM	66-75 nM
V_2	1-800 μM/min	73-167 nM	72-122 nM
k_c	0.1-15	20-158 nM	73-159 nM
k_M^+	0.5-5000 (μM)$^{-3}$min^{-1}	20-81 nM	34-147 nM
k_M^-	80-2000 min^{-1}	68-157 nM	20-255 nM
k_N^+	0.5-500 (μM)$^{-1}$min^{-1}	21-221 nM	16-145 nM
k_N^-	0.5-50 min^{-1}	34-146 nM	21-221 nM
$[CaM_{total}]$	5-500 μM	21-194 nM	27-146 nM

$[CaN_{total}]$	5-500	21-222 nM	27-140 nM
d	0.1-5000 min^{-1}	74-159 nM	70-159 nM
f	0.0001-10 min^{-1}	70-159 nM	78-159 nM
N	4-15	53-161 nM	74-159 nM
λ	0.001-10	61-159 nM	95-159 nM

2.4 Discussion

From Fig. 2.2a and Fig. 2.2b, we can see that when the simulated medium calcium level ($[Ca_{ex}]$) ranges from 1μM to 100mM, the simulated cytosolic calcium ion level of our model cell rests within 73-159nM. Further tests show that the above simulated resting levels are independent of the initial conditions. In normal real yeast cells the cytosolic calcium ion concentration rests within 50-200nM when medium calcium level ranges from < 1μM to > 100mM [145]. The resting levels of our model cell agree with those of real cells.

As mentioned above, when the simulated medium calcium level ($[Ca_{ex}]$) ranges from 1μM to 100mM, the simulated resting level of calcium ion-bound calmodulin remains under a level of 0.5μM. By noting that in the model the total concentration of calmodulin $[CaM_{total}]$ is put to be 25μM (see Table 2.1), we can conclude that the absolute majority of calmodulin molecules are in calcium ion-free form when our model cell is resting. When the simulated cytosolic calcium ion level ($x(t)$) is elevated, calmodulin senses this elevation and quickly binds calcium ion to activate calcineurin (see Fig. 2.3a, Fig. 2.3b and Fig. 2.3c). Such behavior of calmodulin is in accordance with the relevant knowledge presented in literature [53].

By comparing this experimental curve (WT curve in Fig. 2.2d) with the corresponding $x(t)$ curve (Fig. 2.2c) of the model cell, we can find that the general shape of two curves is in accordance: cytosolic calcium ion concentration rises and falls due to the extracellular stimulus. As to the amplitude, the peak value of the experimental (WT) curve in Fig. 2.2d is equivalent to ~260nM [146]. The amplitude of our model response curve (its peak value is around 1.2μM) is in the same order of that of the experimental curve. By depicting the $x(t)$ curve of the model cell in a range of two minutes after the disturbance (Fig. 2.3a) and making the comparison with Fig. 2.2c again, we find that the general part (30-120 seconds after the disturbance) is in agreement with that of the experimental curve: the cytosolic calcium ion level gradually decreases to a new low resting value. Actually a remarkable difference exists in the widths of response spikes. This effect will be explained in Chapter 3.

From Fig. 2.4a, we can see that in low calcium media, our model *PMC1* null mutant cell can achieve calcium homeostasis very well, although this ability is a bit compromised

compared to that of the simulated wild type cell (Please note that for $[Ca_{ex}] = 6\mu M$, the resting $x(t)$ level of our model wild type cell is 76nM whereas the resting $x(t)$ level of our model *PMC1*Δ cell is 82nM). From Fig. 2.4b, we can see that in high calcium media, the simulated cytosolic calcium level is out of control and our model *PMC1*Δ cell must die since calcium homeostasis is vitally important for cell viability. Further tests show that this behavior is basically independent of the initial conditions. These results suggest that our simulated *PMC1*Δ cell exhibits the similar basic characteristic which has been experimentally found in real *PMC1*Δ cell: it is viable in low calcium media and fails to grow in media containing high levels of calcium ion [50].

Robustness is an essential property of biological systems [16,119]. The main phenomenological property exhibited by robust systems is parameter insensitivity which means that the system is relatively insensitive to specific kinetic parameters. In Fig. 2.4c, we can see that when large impulse-like disturbance is imposed on a certain rate constant of our model system, the simulated cytosolic calcium ion level changes slightly and the system quickly recovers to its original resting level when the disturbance is over. In Fig. 2.4d, we can see that in general the value change of N will not have much influence on resting levels. For example, when $N = 4$, the model cell will rest within 53-161nM with parameter $[Ca_{ex}]$ ranging from 1μM to 100mM. When $N = 15$, the model cell will rest within 74-159nM. These ranges of the simulated resting levels are in accordance with the experimentally found range of 50-200 nM. This indicates that our previous discussions of resting levels are not only applicable for only one specific value $N = 13$, but also can apply to other values of N. We can show that our previous discussions of the other behavior of our model cell such as response curves, mutant behavior and robustness are valid for any reasonable value of N. From Table 2.2, we can see that the behavior of our model cell (Eqs. 2.2, 2.4, 2.8, 2.17) exhibits a large degree of insensitivity for almost every parameter except those reported ones. As for parameter V_3, when it ranges from 0 to 10000μM/min, the system always rests within 76-159nM for $[Ca_{ex}]$ ranging from 6μM to 100mM and small oscillations are occasionally observed for $[Ca_{ex}]$ ranging from 1μM to 6μM. Since these small oscillations are bound between 30-150nM and they only occur for a small range of $[Ca_{ex}]$ values, they have limited influence on the effectiveness of our model. All these results show that the feedback control mechanism in our model cell is robust.

The simulation results of our model cell show that tightly controlled low cytosolic calcium ion level can be very natural under the general mechanism of gene expression feedback control (see Fig. 2.2a, Fig. 2.2b and Fig. 2.2c). The calmodulin (a sensor protein) behavior in our model cell agrees well with observations in actual cells (see Fig. 2.3a, Fig. 2.3b and Fig. 2.3c). Our model can qualitatively reproduce the reported response curve of real yeast cells responding to step-like disturbance in media calcium ion level (see Fig. 2.2c and Fig. 2.2d). Our model mutant cell such as *PMC1* null mutant can exhibit some basic characteristic similar to that of real mutant cells (see Fig. 2.4a and Fig. 2.4b). Moreover, the feedback control mechanism in our model is shown to be robust (see

Fig. 2.4c, Fig. 2.4d and Table 2.2). Our model cell exhibits a homeostatic behavior similar to that of real yeast cells, whose main characteristic is robust ``perfect'' adaptation.

On the other hand, we have to realize that this is a relatively coarse model. For example, in the current model, we assume that the concentrations of Pmc1 and Pmr1 are directly proportional to the quantity of transcriptionally active Crz1 (Eqs. 2.11, 2.12). This is a big simplification since in real cells, this process involves the increased gene expression through Crz1 followed by translation and trafficking of the proteins to the respective intracellular destinations [5]. The existence of unknown factors further puts limitations on our model. Besides the unknown mechanism through which Vcx1 is regulated by activated calcineurin, recently some other factors such as Rcn1 [100,111], Mck1 [100] and an ER-localized ATPase Cod1/Spf1 [47] have been shown to play certain roles (although not major roles) in yeast calcium homeostasis. Moreover, the current model does not include the influence from other relevant pathways whereas in real cells, any response to given extracellular stimulus is likely to be the result of complex cross-talk between multiple pathways [184]. For example, it has been reported that intracellular glucose 1-phosphate and glucose 6-phosphate levels modulate calcium homeostasis in yeast cells [4] which means that the glucose metabolism pathway is coupled with the pathway of calcium homeostasis.

The coarseness of our model determines that there are certain discrepancies between our model cell behavior with the behavior of real cells. For example, for our model *PMC1* null mutant cell, the transition point on which the system transits from having a reasonable resting level to having no physiologically reasonable resting level is around 60μM, which is much lower than that of real *PMC1*Δ cell transiting from being viable to being inviable (about 200mM, [50]). As mentioned in Section 2.3.2, the response curve of our model *VCX1Δ* cell (data not shown here) is almost identical to that of the simulated wild type cell (Fig. 2.2c) whereas from Fig. 2.2d, we can clearly see that in the case of real cells, there are distinct differences between the experimental response curve of *VCX1*Δ cell (*VCX1*Δ curve in Fig. 2.2d, its peak value is equivalent to ~360nM [146]) with that of the wild type cell (WT curve in Fig. 2.2d, its peak value is equivalent to ~260nM [146]). Moreover, there are published data indicating that *PMC1* mRNAs accumulate and peak over the course of 10 to 30 minutes before declining when yeast cells are dealt with 100mM extracellular calcium media (see Fig. 2B in Ref. 100). From Fig. 2.3d, we can see that for our model cell, transcriptionally active Crz1 (thus also *PMC1* mRNAs according to our model assumption) accumulate over the course of 10 to 20 minutes. So our model can explain the accumulation and the corresponding time scale is comparable. However, it can not explain the final decline as shown in Fig. 2B in Ref. 100.

We should note that this model is built for log-phase yeast cultures grown in standard synthetic or YPD medium at about 26-30 ^{0}C [50,51,63,132,145,146,150,215]. For yeast cultures grown in very poor media or for yeast cultures out of the log-phase, the current model will possibly not be valid anymore because the dilution effect caused by cell growth may become too small to prevent the saturation of the inexchangeable pool - the vacuole. For example, if the growth rate is zero, for $[Ca_{ex}] = 100mM$, according to our

model, the cytosolic Ca^{2+} will rest at 159nM, and the total steady flux through Pmc1 and Vcx1 should be $941\mu M/\min * Vol$. We can calculate the characteristic time of vacuolar Ca^{2+} saturation by $t_{vac} = 200mM/(941\mu M/\min * (Vol/V_{vac})) = 1063$ min which means after about 18 hours, the vacuole will eventually be saturated for non-growing cells (Please note that here we assume the maximum possible Ca^{2+} concentration in the vacuole to be 200mM).

To conclude, we have built the first preliminary mathematical model to describe calcium homeostasis in growing yeast cells under normal conditions. It provides the first quantitative example exploring the consequences of changes in the quantity of Ca^{2+}-pump and exchanger due to the expression of the protein-encoding genes that follows Ca^{2+}-dependent signal cascade. Such exploration is partially supported by the experimental evidence [100]. The model can correctly predict the different phenotypes of different mutant cells like *PMC1*Δ and *VCX1*Δ. It gives the first quantitative explanation that *PMC1* null mutant's failure to grow in media containing high levels of Ca^{2+} is possibly due to its inability of achieving calcium homeostasis. With this model, we can test and verify theoretical hypotheses by comparing simulation results with corresponding experimental results and generate new hypotheses on the regulation of calcium homeostasis. On the other hand, due to the existence of unknown factors and the lack of experimental data, this model is not an exact model yet. However, it does can give some quantitative insight into the possible dynamics of the whole process and provide a general framework for more elaborate investigations. As we will see in Chapter 3, in order to make it compatible with some new experimental findings, we will revise and extend this preliminary model and develop a new mathematical model to simulate the cytosolic calcium dynamics of *yvc1 cch1* yeast cells in response to hypertonic shock.